

PERCEPTUAL WATERMARKING USING A WAVELET VISIBLE DIFFERENCE PREDICTOR

Xingliang Huang and Bo Zhang

Department of Computer Science & Technology
Tsinghua University, Beijing 100084, P.R.China
hxliang98@mails.tsinghua.edu.cn, dcszb@mail.tsinghua.edu.cn

ABSTRACT

This paper proposes a new pixel-wise perceptual mask based on a wavelet visible difference predictor (WVDP) for watermarking. The mask is very effective that the embedding energy can be sufficiently exerted, and that the annoying global parameter controlling the watermark strength as in usual schemes can be dropped off. The watermark sequence is drawn from a uniform distribution and added to all the detail bands after being masked. In the detection phase, a correlation detector is used, and the original image is not required. Experimental results show that our scheme provides very good performance both in terms of watermark unobtrusiveness and robustness.

1. INTRODUCTION

Watermarking has been proposed to be a possible solution for copyright protection of digital information and great advances in technical aspect have been made. Today it is widely accepted that unobtrusiveness and robustness are both essential requirements of robust watermarking [4], [5]. To ensure that the watermark is unobtrusive, the embedding energy has to be limited under a comparatively low level. However, with more energy there is more room to improve robustness of the watermark. The conflict of these two features prompts the adoption of characteristics of the human visual system (HVS), which has been extensively studied [3] and actively employed in image compression and image quality discrimination [8]-[10].

The Discrete Wavelet Transform (DWT) that operates in a similar way as the multiple channels of the HVS has been proved to be one of the most powerful techniques for image processing. A variety of DWT-based watermarking schemes integrating models of the HVS have also been proposed in the last several years. In [4], the model of [7] is

used: a static weight is determined, based on typical viewing conditions, for each subband that varies in spatial frequency and orientation, and then the watermark signal is weighed and added to the wavelet coefficients. Thus the HVS is exploited only up to a subband resolution. In [5], Barni *et al.* build a pixel-wise mask based on the work by Lewis and Knowles [10], then they scale the watermark sequence and add it to the largest detail bands. The model used in [5] does not account for variations of viewing condition, and besides, the watermark is inserted only into the first decomposition level, thus can not fully exert the embedding energy. El-Khamy *et al.* [6] calculate the just noticeable distortion (JND) profile for each detail coefficient at each resolution level and orientation using Chou's model [9], in which the JND profiles are originally derived in spatial domain. So this model cannot be incorporated into the DWT domain directly.

In this paper, we present a new perceptual mask that exploits a WVDP [1], [2], which takes into account the fundamental properties of the HVS, and operates directly on DWT coefficients, thus can be easily integrated into a DWT-based watermarking scheme. Based on the WVDP, a pixel-by-pixel mask covering all the detail subbands is built, which allows us to exert almost all the embedding energy to make the watermark more robust to various attacks while retaining invisible. In experiments, the effectiveness of our watermarking method is shown.

2. WATERMARKING USING A WVDP

2.1. Watermark Insertion

We first decompose the host image through DWT into four levels. The wavelet transform used here is the linear-phase 9/7 biorthogonal wavelets which have been widely exploited in image compression [7], [8] and are also used in the WVDP [1]. Let the DWT coefficients be denoted by C_l^θ , where l represents the resolution level at $l \in \{1, 2, 3, 4\}$, and θ indexes frequency orientation as follows: $\{1, 2, 3, 4\} = \{LL, HL, LH, HH\}$, where low and high are in the order horizontal-vertical. The watermark consists of a pseudorandom sequence drawn uniformly from the interval

This work is supported by National Nature Science Foundation of China (60135010, 60321002) and the Chinese National Key Foundation R & D Plan (2004CB318108).

$[-1, 1]$. The reason for selecting such a distribution will be made clear in section 2.2. The DWT coefficients at all the detailed subbands, i.e., only excluding the coarse band, are modified to embed the watermark:

$$\tilde{C}_l^\theta(i, j) = C_l^\theta(i, j) + w_l^\theta(i, j)m_l^\theta(i, j), \quad (1)$$

$$l=1, 2, 3, 4, \theta=2, 3, 4,$$

where \tilde{C}_l^θ refers to the watermarked DWT coefficients, m_l^θ is the watermark sequence, and w_l^θ corresponds to the computed local perceptual weight exploiting the masking characteristics of the HVS. It is suggested by experimental tests that not to modify the low pass band, as it can better preserve the watermark invisibility, and, further, it is sufficient for all the detail subbands to cover nearly all the embedding energy. As mentioned above, a global parameter controlling the watermark strength [5], [6] is no longer needed in the embedding rule.

2.2. Perceptual Masking

Bradley describes a WVDP which can reliably predict visual difference between an original and noisy image directly from the wavelet coefficients [1]. Here we take the inserted watermark as the noise in Bradley's model, and then use the WVDP to predict the maximum difference that we can introduce into the DWT coefficients, thus build a mask that takes account of the local noise sensitivity of the human eyes for watermark embedding in the DWT domain. Bradley's model mainly considers these fundamental properties of the HVS: frequency sensitivity, signal content sensitivity, and psychometric function and probability summation. Some modifications of Bradley's model will be introduced in order to better fit the model into the watermarking system.

The frequency sensitivity of the HVS is not explicitly modeled in the WVDP. Instead, a threshold elevation function [3] is built to implicitly account for this property. The threshold elevation function consists of two parts: a minimum threshold when there is little or no contrast masking and an increasing masking function of image contrast. The minimum of the threshold elevation function is based on the psychovisual quantization experiments of [7] and is modeled as follows:

$$\log(n_c(l, \theta)) = \log(a) + k \cdot (\log(f) - \log(g_\theta f_0))^2 - \log(q_\theta) - 2(l-1)\log(p_L), \quad (2)$$

where n_c denotes the coefficient detection threshold, and f is the spatial frequency determined by both viewing conditions and wavelet level, calculated as $f = r \cdot 2^{-l}$ cycles/degree [7], where r is the viewing resolution in pixels/degree. Other constants in (2) take values as $a=0.495$, $k=0.466$, $f_0=0.401$, $g_\theta=1.501$, 1, and 0.534, and q_θ is p_L^2 , $p_L \cdot p_H$, and p_H^2 , for the LL, HL/LH, and HH subbands, respectively. For the linear-phase 9/7 wavelets, we have $p_L=0.788486$ and $p_H=0.852699$.

The minimum threshold, n_c , accounts for the masking effect only up to a subband resolution. The complete masking function, which must also take account of the signal content sensitivity, i.e., the masking effect due to the actual value of the DWT coefficients, C_l^θ , is given by:

$$T_e(l, \theta, i, j) = \max\{n_c(l, \theta), b(l) \cdot \|C_l^\theta(i, j)\|\}, \quad (3)$$

where b is necessary in the case of the critically sampled DWT to reflect the fact that coefficients at higher levels represent decreasing resolutions and therefore have a reduced masking effect [2]. Typical values for four-level decomposition are: $b(l)=4.0, 2.0, 1.0, 0.5$, for $l=1, 2, 3, 4$, respectively [2].

The threshold elevation function T_e and the coefficient differences ($\Delta C_l^\theta(i, j) = C_l^\theta(i, j) - \tilde{C}_l^\theta(i, j)$) are used against the psychometric function [3] to calculate a detection probability for each coefficient in every subband:

$$P_b(l, \theta, i, j) = 1 - \exp\left(-|\Delta C_l^\theta(i, j)/(T_e(l, \theta, i, j) \cdot \alpha)|^\beta\right), \quad (4)$$

where $\beta=2.0$, and $\alpha = 1/(-\ln(1-0.5))^{1/\beta}$.

The detection probability summation is given by:

$$P_d(i, j) = 1 - \prod_{l=1}^4 \prod_{\theta=2}^4 (1 - P_b(l, \theta, i, j)), \quad (5)$$

where P_d is the total probability of detection resulting from all bands as a function of the location of every pixel in the spatial domain.

For our watermarking scheme, we set $P_d=0.5$ which corresponds to one JND. Noticing that there are totally $3L$ detail subbands for L -level wavelet decomposition, the coefficient detection probability is determined with (5) by:

$$P_b(l, \theta, i, j) = 1 - (1 - 0.5)^{-3L}. \quad (6)$$

Combining (4) and (6), we get the predicted JND, i.e., the perceptual weight, for every DWT coefficient:

$$w_l^\theta(i, j) = (3L)^{-1/\beta} \cdot T_e(l, \theta, i, j). \quad (7)$$

From the above, we can see that the perceptual weighing function is derived originally from Watson's model [7] which accounts for uniformly distributed noise over $[-1, 1]$. Therefore, the uniform distribution for generation of watermark sequence was selected.

2.3. Watermark Detection

As usual, a correlation detector without referring to the original image as described in [5] is used. In particular, the correlation is calculated as:

$$\rho = \frac{1}{N} \sum_{l=1}^4 \sum_{\theta=2}^4 \sum_{i,j} \tilde{C}_l^\theta(i, j) m_l^\theta(i, j), \quad (8)$$

where N represents the number of all the DWT coefficients in detail subbands, i.e., the length of the watermark sequence.

To determine the detection threshold T_ρ , just the worst case that the image is watermarked with a watermark n_i^θ other than the test watermark m_i^θ is needed to be considered [5]. It is assumed that ρ is normally distributed, and C_l^θ ($l \in \{1, 2, 3, 4\}$, $\theta \in \{2, 3, 4\}$) is zero-mean independent random variable [5]. Observing that C_l^θ and m_i^θ are independent, and that m_i^θ is uniformly distributed over $[-1, 1]$, the mean and variance of ρ under the worst case (denoted by ρ_w) can be computed as $\mu_{\rho_w} = 0$ and

$$\sigma_{\rho_w}^2 = \frac{\sigma_m^2}{N^2} \sum_{l=1}^4 \sum_{\theta=2}^4 \sum_{i,j} \left(E(C_l^\theta(i, j)^2) + \sigma_m^2 E(w_l^\theta(i, j)^2) \right), \quad (9)$$

respectively, where σ_m^2 is the variance of m_i^θ . Recalling the insertion rule stated in (1), we can find that:

$$E(\tilde{C}_l^\theta(i, j)^2) = E(C_l^\theta(i, j)^2) + \sigma_m^2 E(w_l^\theta(i, j)^2), \quad (10)$$

then we have:

$$\sigma_{\rho_w}^2 = \frac{\sigma_m^2}{N^2} \left(\sum_{l=1}^4 \sum_{\theta=2}^4 \sum_{i,j} E(\tilde{C}_l^\theta(i, j)^2) \right), \quad (11)$$

with which we can use the unbiased estimate of $\sigma_{\rho_w}^2$ in practice:

$$\sigma_{\rho_w}^2 \approx \frac{\sigma_m^2}{N^2} \left(\sum_{l=1}^4 \sum_{\theta=2}^4 \sum_{i,j} \tilde{C}_l^\theta(i, j)^2 \right). \quad (12)$$

Let's denote the probability of false detection by P_f , then we can force that [5]:

$$P_f \leq \frac{1}{2} \operatorname{erfc} \left(\frac{T_\rho}{\sqrt{2\sigma_{\rho_w}^2}} \right), \quad (13)$$

thus T_ρ is determined.

3. EXPERIMENTAL RESULTS

In the experiments that follow, we set that $r=32$ pixels/degree (which corresponds to typical office viewing of desktop computer images [7]), and impose that $P_f \leq 10^{-8}$ (thus we have $T_\rho = 5.615\sigma_{\rho_w}$ [5]).

First, the watermark unobtrusiveness is tested. The original test image *Lena* and its watermarked version are showed in Fig. 1(a) and Fig. 1(b), respectively. Fig. 2(a) is the watermark signal, i.e., the difference between the original image and the watermarked one, from which we can see that the watermark is very structured, taking advantage of the local characteristics of the image. Fig. 2(b), (c), and (d) further illustrate the orientation-adaptive properties of our masking model: Fig. 2(b), which is the perceptual weights for the HL subband at the first decomposition level, demonstrates strong masking effect along horizontal direction, and Fig. 2(c) and (d) indicate strong vertical and diagonal masking, respectively.

To verify that our scheme can better exert embedding



Fig. 1. (a) Original image. (b) Watermarked image.

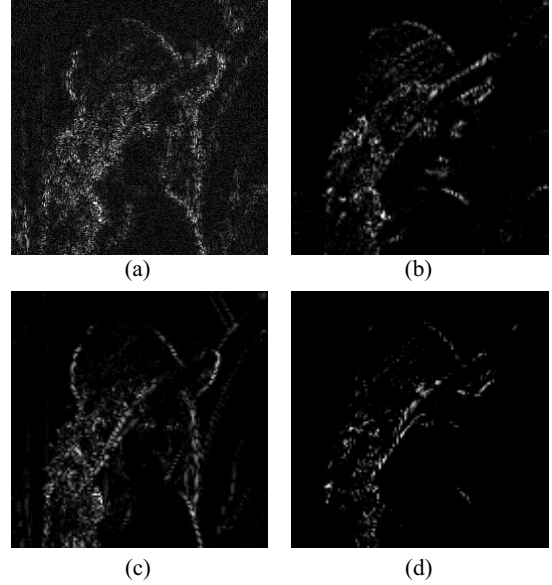


Fig. 2. (a) The watermark: absolute difference between the original image and its watermarked version. (b) Perceptual weights for the HL, (c) LH, and (d) HH subbands at the first level, respectively. Fig. 2(a) ought to be double size of Fig. 2(b), (c) and (d), but here we scale them to be the same size for the convenience of display, and all the figures have been magnified to be visible.

energy, we compare our results with that of two standard masking techniques, [4] and [5]. The quality metrics used here are PSNR and weighed PSNR (wPSNR). The wPSNR metric is implemented in the well-known benchmarking suite, Checkmark [10], taking account of properties of the HVS. We set the watermark strength for each algorithm so that the wPSNRs of the watermarked images are approximately the same, i.e., with the same perceptual quality. Then, we apply the PSNR metric to find out how much watermark energy has been embedded (specifically, the lower the PSNR, the higher the embedded energy is). The results obtained on various standard images are reported in Table 1, which prove the effectiveness of our method.

The robustness of the proposed technique against standard lossy compression coding distortion, such as JPEG and JPEG2000 (based on JasPer Software [11]), is

Table 1. Comparisons of embedding energy (indicated by PSNR) under the same visual quality (indicated by wPSNR).

Test Image	Quality Metric	Our Scheme	Podilchuk & Zeng's Scheme	Barni <i>et al.</i> 's Scheme
Lena	PSNR	32.939	33.024	34.592
	wPSNR	37.041	37.032	37.025
Baboon	PSNR	29.540	30.045	31.558
	wPSNR	37.504	37.492	37.519
Camera Man	PSNR	32.886	33.086	34.681
	wPSNR	36.880	36.869	36.892
Fishing Boat	PSNR	30.306	31.284	32.553
	wPSNR	36.464	36.472	36.453
Watch	PSNR	31.591	31.678	33.856
	wPSNR	37.767	37.759	37.771

also evaluated. Different quality factors are set, and then the compression coding is applied to the watermarked image. At the detector side, 1000 different watermarks, among which is the genuine one, are tested against the corresponding threshold. The results along with the highest fake response of the detector are shown in Fig. 3 and Fig. 4. From Fig. 3 we can see that, with JPEG coding, our algorithm can withstand a quality factor of as low as 6%, and that the highest fake response is always lower than the detection threshold and the true response. In the case of JPEG2000 coding, the detector produces correct result until the compression factor reaches 0.2 bpp, and, again, the fake watermarks are successfully distinguished.

4. CONCLUSION

A new perceptual mask for wavelet-based watermarking is presented. Based on the WVDP that considers characteristics of the HVS, we build an effective pixel-wise mask, which covers all the detail DWT coefficients and helps to exert almost all the embedding energy. Also due to the effectiveness of our perceptual mask, the global parameter controlling the watermark strength in the usual insertion rule becomes needless. Experimental results demonstrate that, with the same perceptual quality, our scheme can obtain higher embedding energy compared with other standard wavelet- and HVS-based algorithms, and that the robustness of our scheme is very satisfying.

REFERENCES

[1] P. Bradley, "A wavelet visible difference predictor," *IEEE Trans. Image Processing*, vol. 8, no. 5, pp. 717-730, May 1999.

[2] P. Bradley and X. Li, "A Wavelet Visible Difference Predictor," *Digit. Image Compu.: Tech. & Appl. (DICTA'97)*, pp. 77-82, Auckland, New Zealand, Dec. 1997.

[3] S. Daly, "The visible difference predictor: An algorithm for the assessment of image fidelity," *Digital Images and Human Vision*, A. B. Watson, Ed. Cambridge, MA: MIT Press, 1993, pp. 179-206.

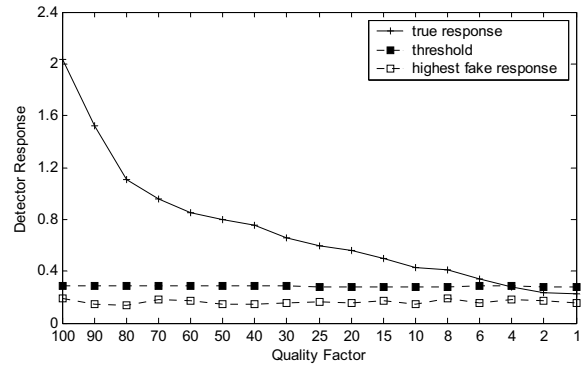


Fig. 3. Robustness test against JPEG coding with decreasing quality factor.

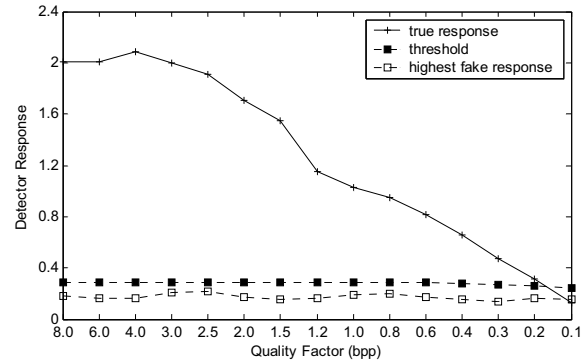


Fig. 4. Robustness test against JPEG2000 coding with decreasing quality factor.

[4] I. Podilchuk and W. Zeng, "Image-adaptive watermarking using visual models," *IEEE J. Select. Areas Commun.*, vol. 16, pp. 525-539, Apr. 1998.

[5] M. Barni, F. Bartolini, and A. Piva, "Improved wavelet-based watermarking through pixel-wise masking," *IEEE Trans. Image Processing*, vol. 10, no. 5, pp. 783-791, May 2001.

[6] S. E. El-Khamy, M. A. Lotfy, and R.A. Sadek, "New technique for perceptual wavelet based image watermarking," *Proc. National Radio Science Conf.*, pp. 336-343, 19-21 March 2002.

[7] A. B. Watson, G. Y. Yang, J. A. Solomon, and J. Villasenor, "Visibility of wavelet quantization noise," *IEEE Trans. Image Processing*, vol. 6, no. 8, pp. 1164-1175, 1997.

[8] S. Lewis and G. Knowles, "Image compression using the 2-D wavelet transform," *IEEE Trans. Image Processing*, vol. 1, pp. 244-250, Apr. 1992.

[9] C.-H. Chou and Y.-C. Li, "A perceptually tuned subband image coder based on the measure of Just-Noticeable-Distortion profile," *IEEE Trans. Circuits & Systems for Video Technology*, vol.5, no. 6, pp. 467-476, Dec. 1995.

[10] S. Pereira, Checkmark Benchmarking Suite. [Online]. Available: <http://watermarking.unige.ch/Checkmark/>

[11] M. D. Adams, JasPer Software. [Online]. Available: <http://www.ece.uvic.ca/~mdadams/jasper/>